Building CT Radiomics Based Nomogram for Preoperative Esophageal Cancer Patients Lymph Node Metastasis Prediction

Chen Shen[*,†,1], Zhenyu Liu[†,1], Zhaoqi Wang[‡,1], Jia Guo[‡], Hongkai Zhang[‡], Yingshu Wang[‡], Jianjun Qin[§], Hailiang Li[‡], Mengjie Fang[†,f], Zhenchao Tang[†,¶], Yin Li[‡], Jinrong Qu[‡] and Jie Tian[*,†,f]

*School of Life Science and Technology, XIDIAN University, Xi'an, Shaanxi, 710126, China; †CAS Key Laboratory of Molecular Imaging, Institute of Automation, Beijing, 100190, China; ‡Department of Radiology, the Affiliated Cancer Hospital of Zhengzhou University, Henan Cancer Hospital, Zhengzhou, Henan, 450003, China; §Department of Thoracic Surgery, the Affiliated Cancer Hospital of Zhengzhou University, Henan Cancer Hospital, Zhengzhou, Henan, 450003, China; ¶School of Mechanical, Electrical & Information Engineering, Shandong University, Weihai, Shandong Province, 264209, China; #University of Chinese Academy of Sciences, Beijing, 100080,China

Abstract

PURPOSE: To build and validate a radiomics-based nomogram for the prediction of pre-operation lymph node (LN) metastasis in esophageal cancer. *PATIENTS AND METHODS:* A total of 197 esophageal cancer patients were enrolled in this study, and their LN metastases have been pathologically confirmed. The data were collected from January 2016 to May 2016; patients in the first three months were set in the training cohort, and patients in April 2016 were set in the validation cohort. About 788 radiomics features were extracted from computed tomography (CT) images of the patients. The elastic-net approach was exploited for dimension reduction and selection of the feature space. The multivariable logistic regression analysis was adopted to build the radiomics signature and another predictive nomogram model. The predictive nomogram model was composed of three factors with the radiomics signature, where CT reported the LN number and position risk level. The performance and usefulness of the built model were assessed by the calibration and decision curve analysis. *RESULTS:* Thirteen radiomics features were selected to build the radiomics signature. The radiomics signature was significantly associated with the LN metastasis ($P<0.001$). The area under the curve (AUC) of the radiomics signature performance in the training cohort was 0.806 (95% CI: 0.732-0.881), and in the validation cohort it was 0.771 (95% CI: 0.632-0.910). The model showed good discrimination, with a Harrell's Concordance Index of 0.768 (0.672 to 0.864, 95% CI) in the training cohort and 0.754 (0.603 to 0.895, 95% CI) in the validation cohort. Decision curve analysis showed our model will receive benefit when the threshold probability was larger than 0.15. *CONCLUSION:* The present study proposed a radiomics-based nomogram involving the radiomics signature, so the CT reported the status of the suspected LN and the dummy variable of the tumor position. It can be potentially applied in the individual preoperative prediction of the LN metastasis status in esophageal cancer patients.

Translational Oncology (2018) 11, 815–824

Address all correspondence to: Yin Li or Jinrong Qu, MD, 127 Dongming Road, Zhengzhou, 450003 or Jie Tian, PhD, Institute of Automation Chinese Academy of Sciences, Beijing 100190, China.
E-mails: liyin825@aliyun.com, qjryq@126.com
[1] Equal contributors: Chen Shen, Zhaoqi Wang, Zhenyu Liu.

Introduction

Esophageal cancer (EC) is the eighth most common malignancy in the world and the incidence is rapidly increasing [1,2]; it is associated with an overall 5-year survival rate of 5% to 20% [3–5]. Surgery remains the only curative treatment with a 5-year survival rate of 34-36% for resectable EC treated with surgery alone, especially for early stage patients [6]. The overall 5-year survival rate after surgery is 70-92% for EC patients without nodal involvement, but only 18-47% for EC patients with lymph node metastasis [7,8].

Surgery approach is dependent on the location of lymph node involvement. The left thoracic approach (Sweet procedure) has merits of a single incision and adequate exposure of the hiatus, but provides insufficient lymphadenectomy in the upper mediastinum. On the contrary, the right thoracic approach (Ivor Lewis procedure) aims to improve the survival by offering a more extended radial lymphad-enectomy. Significantly better 3-year DFS and OS rates among patients who received right thoracic esophagectomy were found, as compared with left thoracic esophagectomy. These benefits were only seen in patients with lymph node involvement and/or positive resection margins, and not in patients without lymph node involvement and negative resection margins [9].

Although the 7th edition of UICC TNM staging has modified the scoring system, it still remains many controversies on the accuracy and reliability of the nodal portion of the TNM staging system. Since some potentially relationships between the critical prognosis information and lymph node (LN) status were omitted [10]. Currently available imaging techniques, endoscopic ultrasound (EUS), Computed tomography (CT), Endobronchial ultrasound (EBUS), 18F-fluorodeoxyglucose positron emission tomography (FDG-PET), and FDG-PET/CT, all have their limitations, and suboptimal imaging quality often leads to an incorrect assessment of regional lymph node involvement [11]. Currently, there are no acceptable guidelines for upstaging the nodal status even though the immunohistochemical analysis has detected the micrometastases.

CT is the most common imaging modality and has a good description of EC tumors. However, identifying the LN metastasis status of EC in CT images is a challenging and meaningful work. Driven by the "big-data" trend, "radiomics" was proposed and then developed rapidly [12]. Because of its non-invasive and low-cost properties, "radiomics" could be regarded as a proper approach for pre-diagnosis assistance. "Radiomics" converts medical images into abstract numerical features, and uses data-mining algorithms for
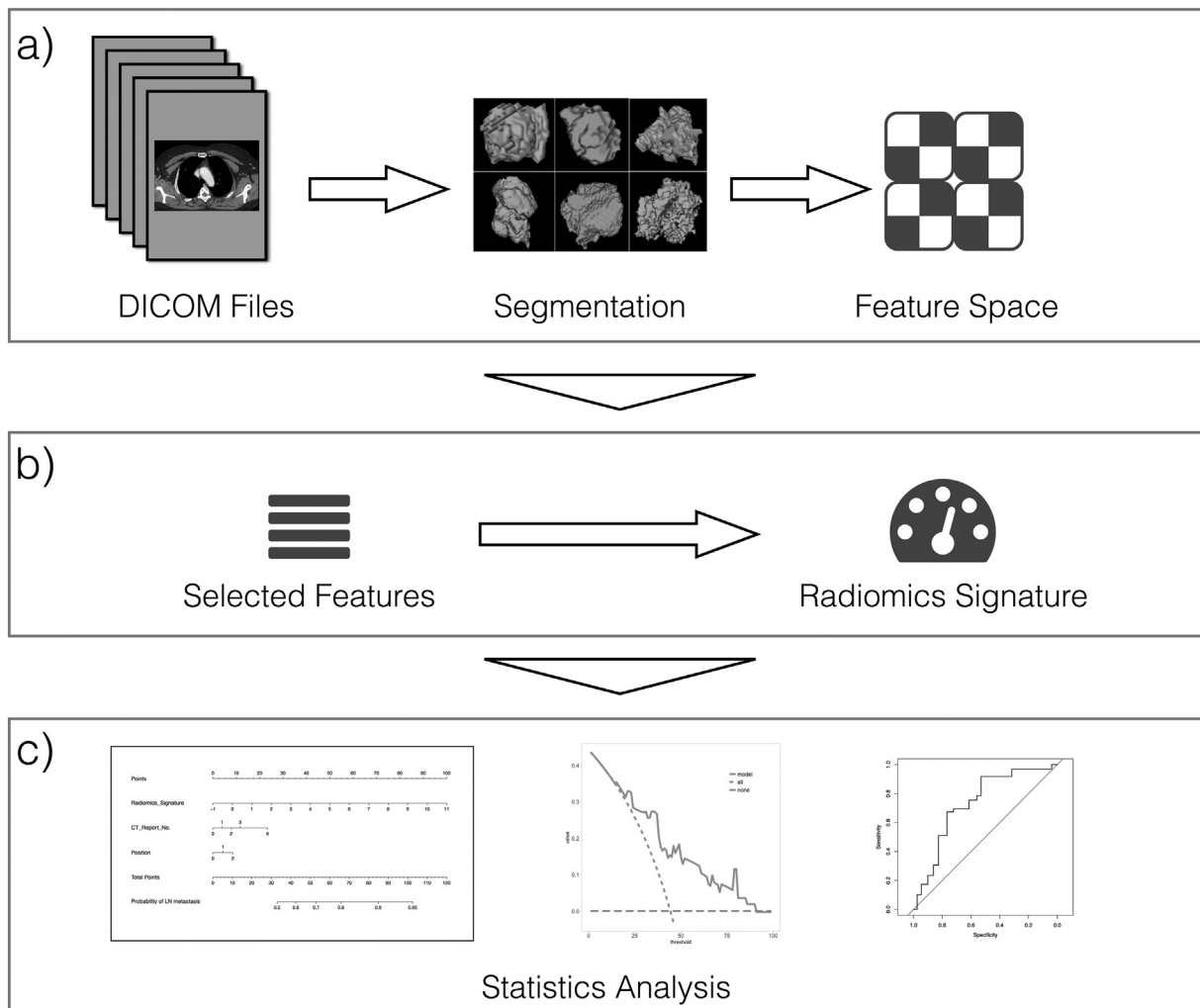
Figure 1. The common process of a radiomics approach. (a) The feature extraction phase, reading the raw DICOM format clinical data and working out the lesion region. All radiomics features will be calculated on those segmentations; (b) the feature analysis phase: select the refined features and build the "radiomics signature"; and (c) the statistical analysis phase: build and assess the nomogram.

analysis. It is desirable to quantify the clinicians' years of experience as a valuable reference [13,14]. It is also known that "radiomics"-based signatures as biomarkers have correlations with clinical stages, LN metastasis, and tumor heterogeneity [15,16]. Radiologists and clinicians started to pay attention and welcome "radiomics" approaches and conclusions in many diseases including CL [17,18].

In this study, we aim to build and validate a radiomics-based nomogram involving radiomics signature and radiological observation factors for the individual prediction of LN metastasis in preoperative esophageal cancer patients. Figure 1 illustrates the flowchart of the research sequence.

Materials and Methods

Patients

In the present study, we enrolled 197 patients with esophageal cancer between January 2016 and May 2016. We collected their pre-treatment CT images and pathologically confirmed the lymph node metastases status. The inclusion criteria we followed are: (a) patients who had collected CT images before any treatment; (b) patients who received lymph node dissection 15 days after the first CT acquisition; and (c) patients who had pathologically confirmed LN metastasis results after the operations. In order to guarantee the consistency of CT and pathological results, 15 days is our criteria because overdue CT images may not reveal the postoperative pathology. The exclusion criteria we followed are: (a) patients who were under 18 years of age; (b) patients who had further treatment (like radiotherapy and chemotherapy); (c) patients who had treatment in other institutes and (d) histological grade was unconfirmed.

Patients were divided into two individual cohorts for the cut-off date of March 31, 2016. The training cohort consisted of patients in the first three months (January to March 2016). The remaining patients (in April to May 2016) formed the validation cohort. Patients' pathological classification, clinical T and N stages were collected from pathological reports directly. We also collected CT reports of the enrolled patients. We extracted the number of metastatic LN and the tumor position in CT reports. Here we defined the semantic feature of the tumor positions depending on the degree of risk (0, 1, and 2 as the lesions in the upper, middle and lower parts of the thoracic esophagus in anatomy). All CT reports were confirmed by two level radiologists' reviews.

Image Acquisitions and Tumor Segmentation

We acquired our images from the Department of Radiology at Henan Cancer Hospital between Jan 2016 and May 2016. We performed the contrast-enhanced CT of Chest on every patient after a 50s delay following intravenous administration of 90 ml of iodinated contrast material (Ousu, Yangtze River Pharmaceutical, Taizhou, China) at a rate of 3.0–4.0 ml/s with a pump injector (Spectris Solaris EP; One Medrad Drive Indianola, PA, USA). Three multi-detector row CT (MDCT) systems were used for acquisition: Phillips 256 iCT, Phillips Medical System; Bright speed 16-slice CT or light speed Pro 32-slice VCT, GE Medical systems, USA. The acquisition parameters were set as follows: 110-120 kV; 168-324 mA; 0.5 or 0.4 s

(a)   (b)

(c)   (d)
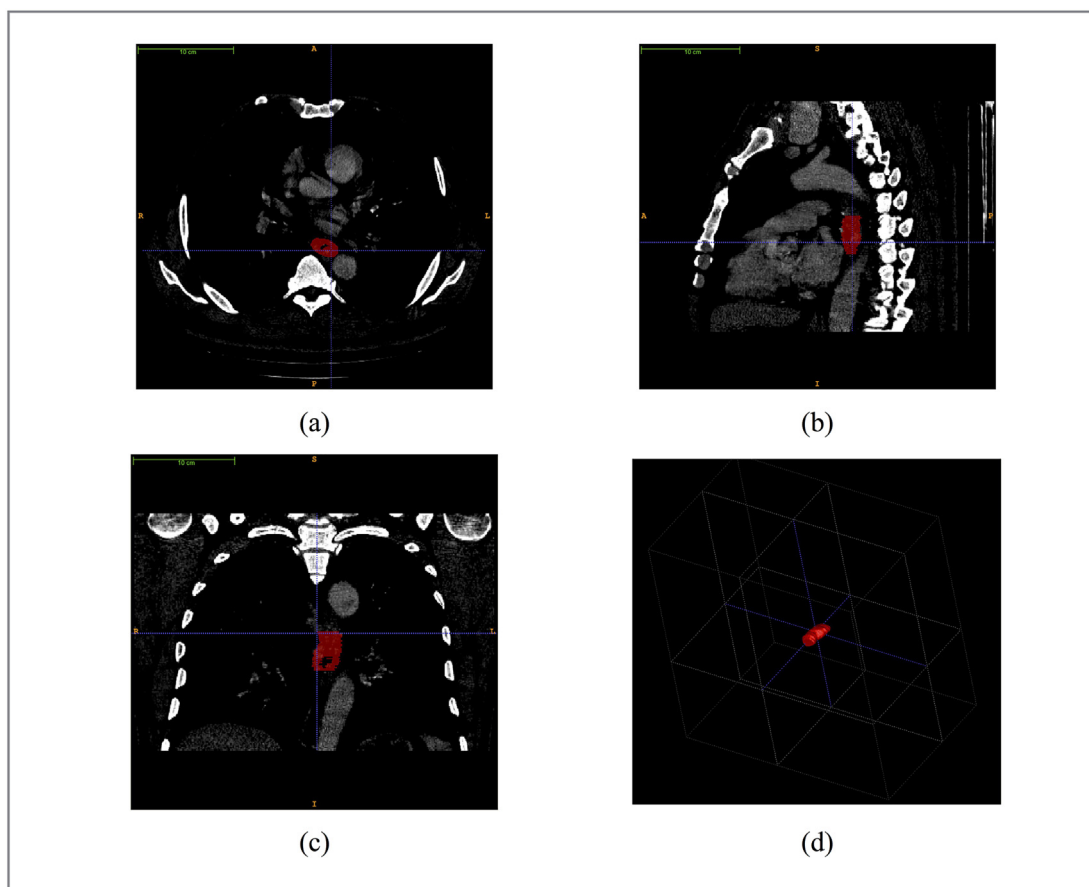
Figure 2. The demonstration of our radiologists working on the tumor segmentation with ITK-SNAP. (a), (b), (c) screenshots of segmentation results in axial, sagittal, coronal planes; (d) the mesh visualization of the lesion sample.

rotation time; detector collimation: 64 × 1.25 mm or 64 × 0.625mm or 16 × 1.25mm or 32 × 1.25mm; field of view, 500 × 500mm; matrix, 512 × 512. Contrast-enhanced CT was performed. All CT images were reconstructed with a standard kernel. These CT images were retrieved from the picture archiving and communication system (PACS) (Neusoft v5.5.60801, Shenyang, China).

Radiologists with over 5 years of experience examined each layer of the patients' CT data. In China, radiologist with over 5 years of experience can have the right to check the report. We performed the manual segmentation of the esophageal tumor on each patient's CT images. We introduced "ITK-SNAP" for this task (www.itksnap.org) [19]. ITK-SNAP is an open-source and free software application used to segment structures in 3D medical images. Two radiologists with more than five years of experience in interpreting chest radiology outlined all of the tumor regions in each patient's CT image layer (Figure 2). These regions of interests (ROIs) would be used in subsequent feature extraction for further analysis.

Radiomics Feature Extraction

Radiomics feature extraction was based on the segmentation results from the previous section. We implemented the calculation through our homemade Matlab scripts (Matlab 2014b, Mathworks, USA). Features included certain categories: first-order histogram statistics, Gray-Level Co-occurrence Matrix (GLCM), Gray-Level Run-length Matrix (GLRL), Fractal Dimensions, and wavelet filtered GLCM and GLRL [20–22]. A total of 788 features were extracted, which covered the major high-throughput radiomics features of current studies. The

details of the radiomics features calculation can be found in the Supplementary Doc. S1.

Radiomics Signature Building

We built the radiomics signature with selected features on the training cohort. The feature selection approach we adopted was the "elastic-net", which is a combination and expansion of the least absolute shrinkage selection operator (LASSO) and the Ridge Regression [23,24]. To screen out the effective and predictable features from high dimensional feature space, ten-fold cross validation was used in the parameters tuning of the "elastic-net". We exploited the logistic regression model to build the radiomics signature for each patient. The radiomics signature is a linear combination of selected features with respective weights, which would be calculated as a factor (radiomics score, Rad-score) for the further prediction model. The assessment method of the logistic regression model is the receiver operating characteristic curve (ROC) and its area under the curve (AUC).

Nomogram Building

The nomogram with the predicting model was based on the multivariable logistic regression analysis. The following candidate factors: CT-reported LN status (dichotomized variable: "0" for no metastasis, "1" for metastasis), CT-reported positions (dummy variable: "0", "1" and "2") and Rad-scores were involved in a diagnostic model for predicting LN metastasis. The nomogram is a graphical representation of this prediction model in the training cohort. It would be tested in the validation cohort.

Table 1. Demographic statistics of patients in the training and validation cohorts

Characteristics		Training cohort			Validation cohort			$P^\dagger$
		LN+	LN-	P	LN+	LN-	P	
		n = 42	n = 98		n = 19	n = 38		0.734
Gender								0.453
	Male	16	51	0.130	12	26	0.769	
	Female	26	47		7	12		
Age								0.919
	Mean	59.5	63.6	0.004*	63.2	62.2	0.660	
	Median	60.0	64.5		63.0	62.5		
	Range	42~74	46~86		50~79	50~75		
	SD	7.4	7.6		7.5	7.3		
Position								0.863
	0	5	13	0.912	3	6	0.827	
	1	20	49		10	17		
	2	17	36		6	15		
T stage								0.372
	1	0	18	0.005*	1	10	0.209	
	2	6	24		5	10		
	3	33	52		12	15		
	4	3	4		1	3		
N stage								0.957
	0	-	98		-	38		
	1	23	-		11	-		
	2	15	-		6	-		
	3	4	-		2	-		
CT Report								0.093
	0	24	65	0.430	15	29	0.970	
Number	1~2	17	29		3	7		
	>3	1	4		1	2		

Note:

P value is calculated from the univariable association test between sub-groups

χ^2 test and Fisher's exact test for categorized variables; two-sample t-test for continues variables

* P value < 0.05

† The comparison between the training cohort and validation cohort

Abbreviations: LN, lymph node; +, metastasis positive; - metastasis negative, CT, computed tomography; SD, standard deviation.

Nomogram Validation

The building of a radiomics nomogram was assessed by calibration curves in both training and validation cohorts. The discrimination power of the predicting model was evaluated by Harrell's concordance index (C-Index) [25]. We used the bootstrap approach for resampling in 1000 times, to calculate the C-index with 95% confidence intervals [26] in both cohorts. The calibration curves were drawn for assessing the agreement between the predicted results and true outcomes of LN metastasis [27]. The decision curve analysis was introduced to evaluate the quantified net benefit of our prediction model in the validation cohort [28].
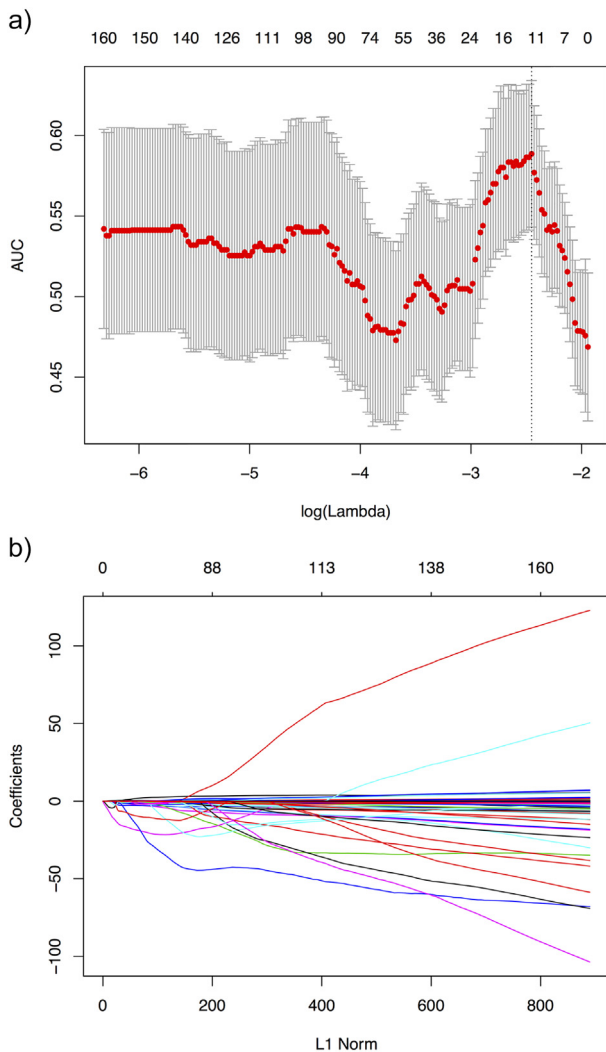
Statistical Tools

We performed the statistical analysis in R (version 3.3.0; http://www.Rproject.org). The used R packages of this paper are listed in the Supplementary Table S1. The statistical significance levels were all

Table 2. Selected Features with Descriptions

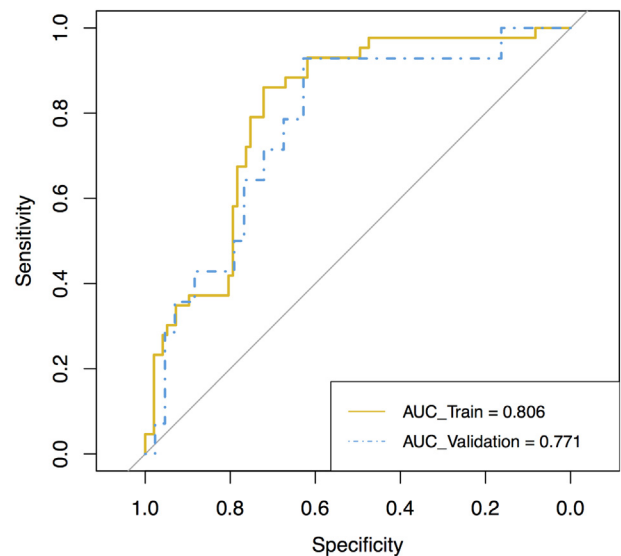| Feature Name	Description
Length	The lesion length measured by the CT layers
Energy	Measure of the overall intensity of the ROI
Kurtosis	Measure of the sharpness of the histogram
GLRL_RLN_45	Measure of the gray scale texture repeatability
a1_GLRL_LRE_135	High dimensional wavelet texture analysis
a1_GLRL_SRHGE_0	
a2_GLCM_PROBABILITY_0	
a2_GLRL_HGRE_0	
a2_GLRL_LGRE_45	
hd_GLRL_SRHGE	
hd_GLRL_SRE_45	
hd_GLRL_SRE_90	
hd_GLRL_SRHGE_135	

Note:
1. prefix of "a1", "a2", "hd" mean the different densities and directions of the wavelet transform performed in Matlab
2. suffix of "0", "45", "90","135" mean the directions of gray-level matrix directions.

set as two-sided at $P = 0.05$ in our report. We assessed the calibration curves with the Hosmer-Lemeshow test. The Hosmer-Lemeshow test is a common statistical test for evaluating the goodness of fit for logistic regression. Common comparisons of patients' characteristics were conducted by a two-sample t-test for continuous variables. Fisher's exact test and χ^2 test were used for categorical variables. The Mann-Whitney U test was utilized for testing the potential correlation of the radiomics signatures and the LN status in both training and validation cohorts. We introduced the inter-observer correlation coefficients (ICCs) to assess the agreement of extracting features by two-level radiologists.


Figure 3. Feature selection using the elastic-net method with a logistic regression model. (a) Tuning parameter λ in the elastic-net model. The parameter λ were selected under the minimum criteria. The vertical line was drawn at the value selected by using 10-fold cross-validation, including optimized 13 nonzero coefficients. (b) The model coefficient trendlines of the 788 radiomics features. The profile graph was plotted by coefficients against the L1 norm (inverse proportional to log λ).

Figure 4. ROCs were employed to assess the radiomics signature discriminative performance of the LN metastasis. ROC in the training cohort with 0.806 (95% CI: 0.732-0.881, sensitivity = 67.9%, specificity = 82.7%); ROC in the validation cohort with 0.771 (95% CI: 0.632-0.910, sensitivity = 76.7%, specificity = 61.2%).
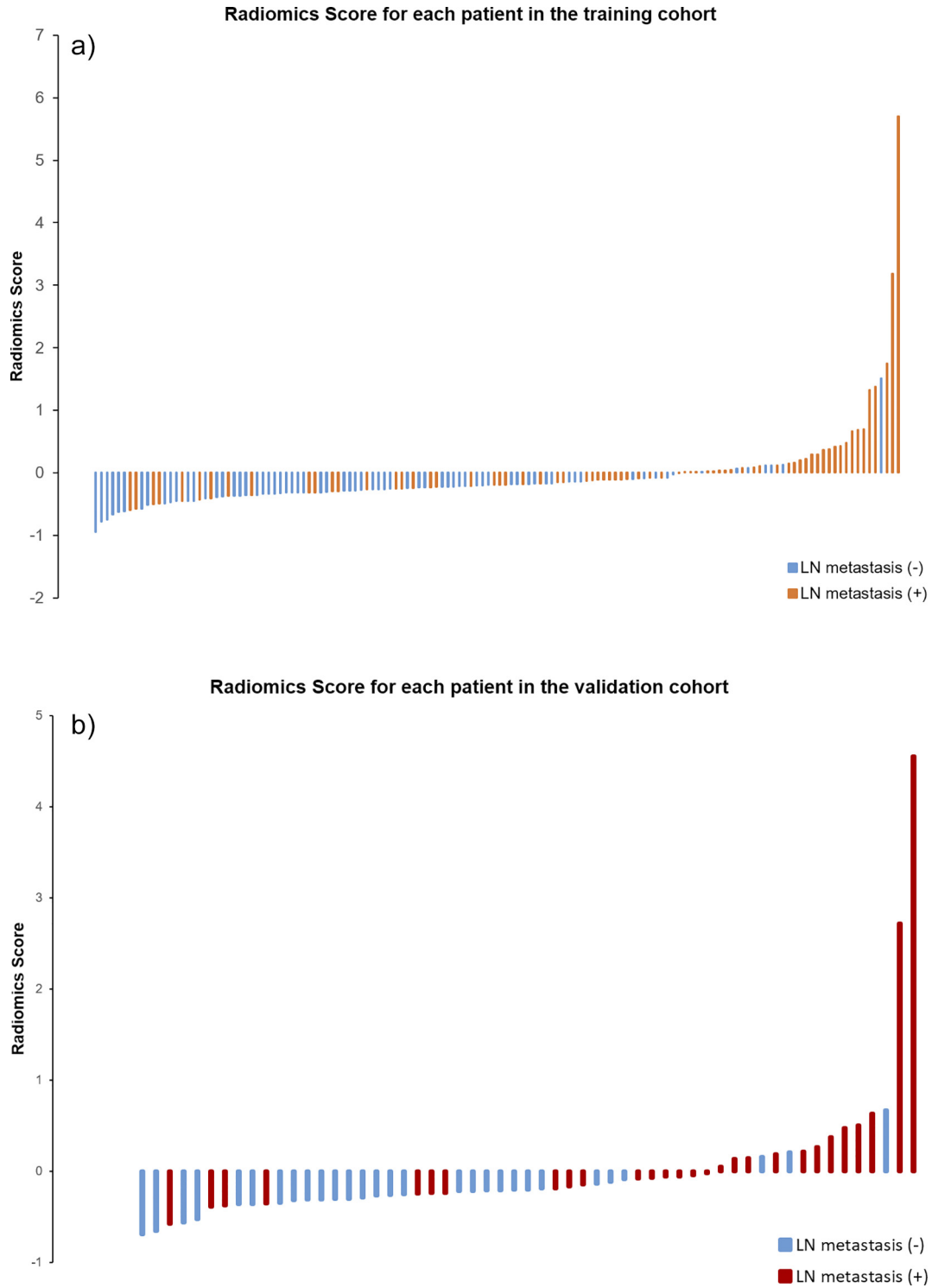
Figure 5. (a): Rad-score for each patient in the training cohort (b): Rad-score for each patient in the validation cohort

Results

Patients' Characteristics

Patients' characteristics with statistics are listed in Table 1. There are 140 patients enrolled in the training cohort and 57 patients in the validation cohort. Two cohorts have no significant difference in the LN metastasis (P = 0.734, χ^2 test). There were no significant differences in other factors. We have found that the accuracy of the CT reported LN metastasis number in our cases was quite low (0.59), and with an extremely high false negative rate (0.64).

Selected Radiomics Features

Based on the elastic-net approach in the training cohort, we selected the features with non-zero coefficients. As a result, 13 radiomics features were screened out from 788 features. Figure 3 illustrates the parameter

Table 3. Results of the Multivariable Logistic Regression

	Coefficient	Odds Ratio	95% CI		P
			Lower	Upper	
Intercept	-1.798				<0.001*
Radiomics signature	0.807	1.255	1.100	1.433	<0.001*
CT Report LN status	0.581	1.788	1.144	2.796	0.046*
Position	0.600	3.323	1.637	6.741	0.002*

Note: * $P < 0.05$.

tuning procedure of the regression model and the feature space reduction. As a result, Table 2 lists the name and description of the selected features. The inter-observer correlation coefficients (ICCs) between two radiologists' agreement is 0.873 (0.758 to 0.921, 95% CI).

Radiomics Nomogram Development

We employed the selected features in the last section to build the radiomics signature, which is the linear combination of the logistic regression model with the selected features. The radiomics signature's discriminative power of the LN metastasis was assessed by two ROCs in the both cohorts correspondingly (Figure 4). Radiomics scores (Rad-scores) of patients were calculated through the elastic-net model with selected features with their corresponding weights. Figure 5 shows each patient's Rad-scores in both the training cohort and validation cohort. We enrolled the Rad-scores, the status of the suspected LNs by the CT report and tumor positions as factors in a multivariable logistic regression analysis to build the personalized LN status prediction model. The coefficients of the model are listed in Table 3. All factors met the significant level, but the "CT Report LN status" was on the edge of significance. Hence, we discarded this factor out of our model. Subsequently, the radiomics-based nomogram was developed by the prediction model (Figure 6).

Validation of the Radiomics Nomogram

We achieved an acceptable calibration in the validation cohort as shown in Figure 7. The Hosmer-Lemeshow test showed that the statistical difference between the calibration curves and the ideal curves was non-significant ($P = 0.541$ for the training cohort and $P = 0.093$ for the validation cohort). The C-index of the radiomics-based nomogram was 0.768 (0.672 to 0.864, 95% CI) for the training cohort and 0.754 (0.603 to 0.895, 95% CI) for the validation cohort. The decision curve analysis (DCA) for the prediction model derived from the radiomics-based nomogram is presented in Figure 8. The DCA showed that our prediction model had a better net benefit than either the treatment or no treatment schemes when the threshold probability was greater than 0.15.

Discussion

In the present study, we developed a predictive model of preoperative EC LN metastasis. The model incorporated three factors: radiomics signature, CT reported suspicious LN number and the tumor position to predict the LN metastasis status. The radiomics signature was significantly associated with the risk of LN metastasis. The nomogram was derived from the prediction model with good calibration and validation. The nomogram has the potential to assist in a preoperative clinical diagnosis, to some extent, which is intuitive to clinicians.

Selecting features from a massive feature pool is the key procedure of a radiomics study. The less useful features can streamline the prediction model and prevent overfitting issues. In this study, 13 features were screened out from the 788 features' pool using the elastic-net approach, which also created a radiomics signature simultaneously through the embedded logistic-regression. According to some statistical modeling reference [29], 13 features of the 197 cases had a proper ratio for building the prediction model that could avoid overfitting. Hence, we found similar ROCs with close AUCs (0.806 and 0.771) in two cohorts of the radiomics signature for the discrimination power of the LN metastasis (Figure 4). The selected
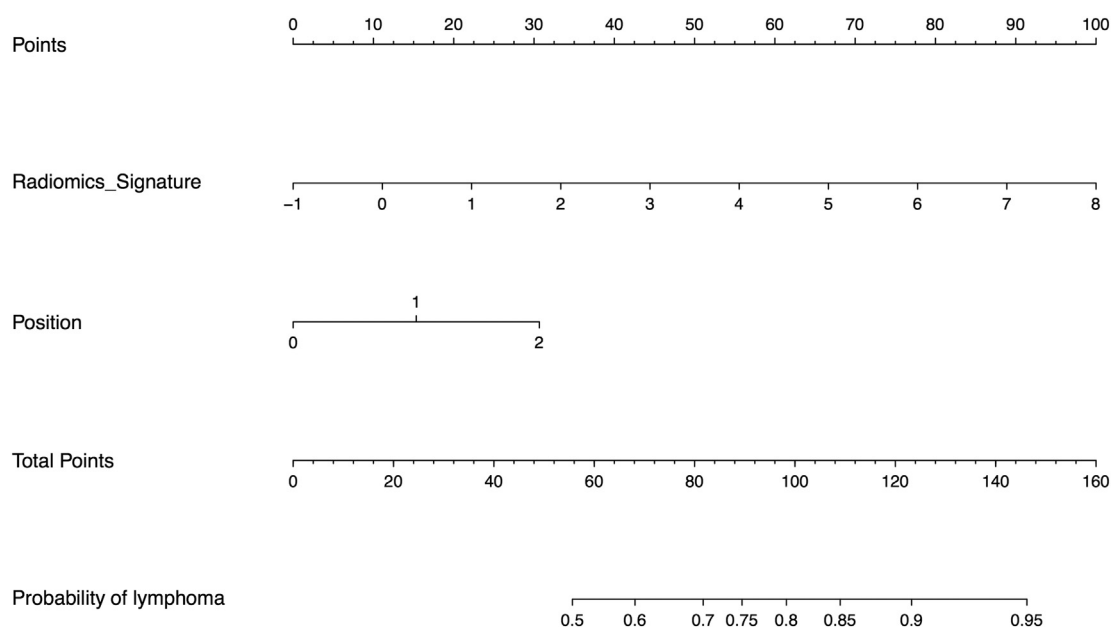
Figure 6. The nomogram of diagnosis model. Our radiomics based nomogram was built in the training cohort. The radiomics signature, CT reported the suspecting lymph node (LN) status and the tumor position (dummy variable) was incorporated as factors.
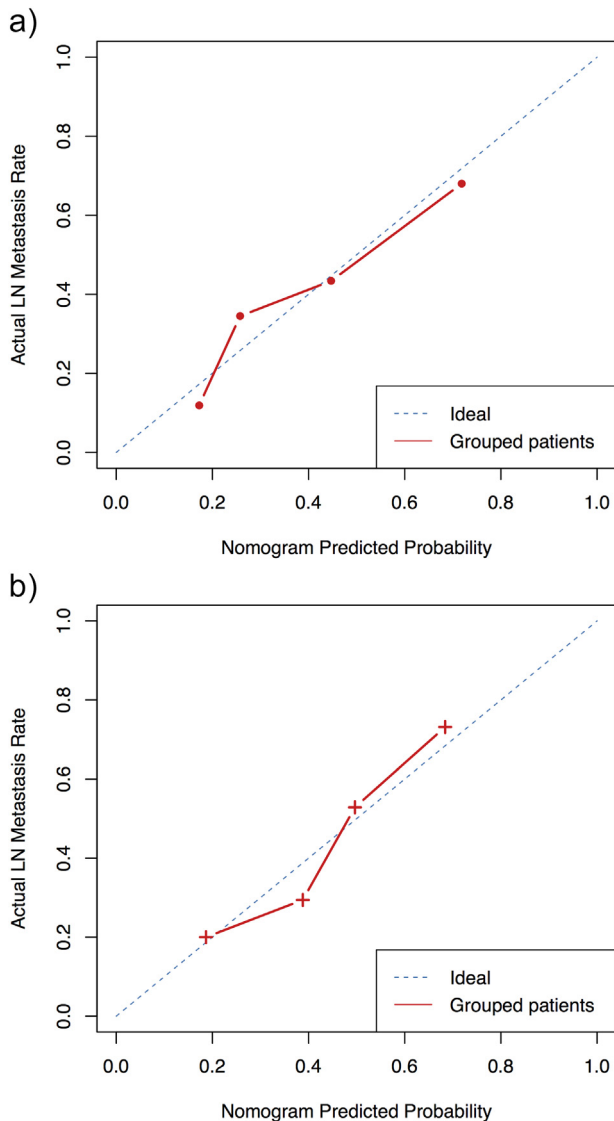
Figure 7. Calibration curves of the radiomics-based diagnosis nomogram. The red dotted line closer to the blue dotted line indicates a better calibration. (a) The calibration curve of the training cohort; (b) the calibration curve of the validation cohort.

radiomics features with a description are listed in Table 2. Features of "Length" and "Energy" are highly consistent with the normal radiological experience, which describes the external contour information of the tumor. The longer length and higher CT enhanced values mean more tumor invasions, hence this leads to higher risk of LN metastasis. These two features can be captured by naked eyes, but our model quantified those experiences into accurate coefficients and factors. The feature of "Kurtosis" is a common measure of a CT gray-level histogram. It often appeared in the early year's medical image post-processing studies. The feature of "GLRL_RLN_45" and the resting wavelet features mainly represent the texture complexity of tumors. Several papers proved that the texture information of tumors is highly associated with the tumors' heterogeneity, and the heterogeneity is closely related to the patient's prognosis [22,30]. Yip et al. introduced this idea into their recent research in EC [18]. Our results supported this view, and we also demonstrated that these features are associated with esophageal cancer LN metastasis. Sequentially, the radiomics signature combined these

multiple imaging features into one biomarker, "Rad-score", involved in a multivariable logistic regression model.

We sorted all patients' Rad-scores with the labeled LN status in Figure 5. It clearly shows that the Rad-score could potentially separate the two types of patients. The corresponding statistical tests have also confirmed that the radiomics signature could be considered as an image-biomarker. The radiomics signature occupied a dominating factor position in our model-derived nomogram, compared to the "Position". It means the radiomics signature has better discrimination power compared to the classical radiologists' perspective. On the other hand, many researches are currently working on various novel prognostic markers for EC patients [31]. Our proposed potential image-based biomarker is preoperative, noninvasive and low-cost. Identification of lymph node metastases on CT imaging is often difficult, especially for nodal micrometastases. In our study, the accuracy of conventional CT evaluation of lymph node metastases was only 0.61 with a false negative rate of 0.66. The meta-analysis supports this low rate result [32]. However, the radiomics signature achieved the AUC over 0.75 (with reasonable sensitivities and specificities), and the accuracy was over 0.8 (Figures 4 and 5). We believe it is a gratifying improvement for non-invasive approaches. Prediction model included the CT reported status and position of conventional CT factors and they also showed the ability of differential diagnosis for the LN status, especially for the position. Some reports showed that the position of the EC was correlated with prognosis, so a dummy variable procedure was used for the risk degree of the position, and it works in the model. A nomogram was built to assist radiologists in providing predictive information by simple scoring, and any other new useful factors could be absorbed into the model to elaborate the model of the nomogram.

Patients without LN metastases (N0) accounted for the majority in our datasets. This is because we take the surgical treatment as the first choice for early stage EC patients (T1 or T2) in China. For advanced patients (T3 or T4), we tend to take the strategy of chemotherapy first and then surgery, those patients are out of the inclusion criteria. The norms maybe different between west countries and the East Asia. West countries normally thought

Controversies is still going on regarding the optimal surgical approach for better patient overall survival. In Western countries, more attention is paied to transhiatal or transthoracic procedures [33,34]. The transthoracic approach is widely used in China, however, the debate between the left and right thoracic approaches is still ongoing. The left thoracic approach shows advantages of a single incision and adequate exposure of the hiatus, but difficulty for sufficient lymphadenectomy in the upper mediastinum. On the contrary, the right thoracic approach aims to increase the survival by offering sufficient radial lymphadenectomy [9], even after several years of being recommended by the Chinese Anti-Cancer Association [35]. Meanwhile, it was reported that extent of lymph node dissection should accord to the incidence of metastasis [36].

A pooled sensitivity of 80% and specificity of 70% of N-staging were reported in a recent meta-analysis including both EUS and EUS-FNA studies [32]. Both understaging (3 %) and overstaging (25 %) of lymph node involvement were reported [37]. A study that compared EUS (without FNA) with FDG-PET and CT found that the accuracy of EUS was not significantly higher than FDG-PET or CT (75%vs. 66%and 63 %, respectively, $P > 0.05$) [38]. Similar results were found in a third study where the accuracy of EUS in diagnosing lymph node metastases was 65 % and only 44 % for
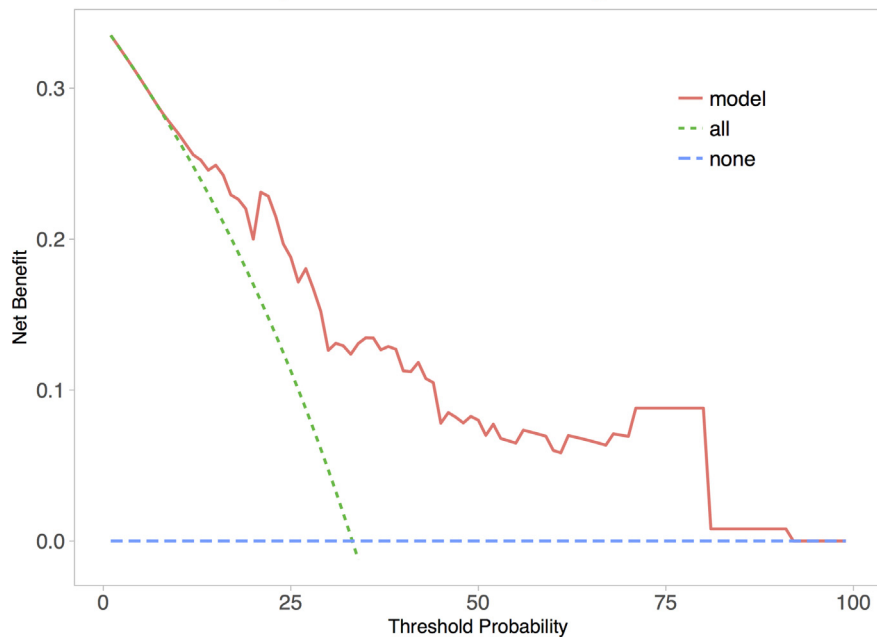
Figure 8. The decision curve analysis (DCA) of the radiomics-based nomogram. The blue line describes the scheme of no treatment. The green line describes the scheme of treatment. The red line represents our personalized prediction model. The x-axis is the threshold probability and the y-axis is the net benefit. The decision curve shown by the pink line (our prediction model) received more net benefit when the threshold probability was larger than 0.15. Hence, if the patient would choose the treatment when his probability of cancer was larger than 15%, then he would receive benefit from taking our radiomics-based nomogram guidance.

small-sized lymph node metastases (<1 cm) [39]. Likewise, the limited value of CT in determining lymph node status is indicated by a meta-analysis reporting a sensitivity of 50 % (95% CI 41–60 %) and specificity of 83 % (95% CI 77–89 %) [32]. Regarding FDG-PET in the assessment of regional lymph node metastases, a meta-analysis revealed a poor pooled sensitivity of 51 % (95% CI 34–69 %) and specificity of 84 % (95% CI 76–91 %) [40].

Limitations of the present study include three aspects. First, the amount of dataset information is inadequate. Commonly, a larger amount of data will improve the confidence and performance of our model. Second, there was only one imaging modality in our study involving dynamic contrast enhanced images and more image modalities, such as MRI, which will expand the feature pool and may find more valuable radiomics features. Finally, the genomic information was not considered in our study. Currently, many works are seeking the correlation between genetic markers and image features so-called "radio-genomics".

Acknowledgement

Disclosure Statement
This retrospective study was approved by the institutional review board of the Affiliated Cancer Hospital of Zhengzhou University, Henan Cancer Hospital, which waived the requirement for the patients' informed consent. Medical record review was performed in accordance with the institutional ethics review board guidelines. All authors had full access to all of the data in the study and had final responsibility for the decision to submit for publication. All authors has no conflict of interest.

Appendix A. Supplementary data
Supplementary data to this article can be found online at https://doi.org/10.1016/j.tranon.2018.04.005.

References

[1] Enzinger PC and Mayer RJ (2003). Esophageal cancer. *N Engl J Med* **349**(23), 2241–2252.

[2] van Hagen P, et al (2012). Preoperative chemoradiotherapy for esophageal or junctional cancer. *N Engl J Med* **366**(22), 2074–2084.

[3] Kumbasar B (2002). Carcinoma of esophagus: radiologic diagnosis and staging. *Eur J Radiol* **42**(3), 170–180.

[4] Siegel R, Naishadham D, and Jemal A (2012). Cancer statistics for hispanics/latinos, 2012. *CA Cancer J Clin* **62**(5), 283–298.

[5] Tanaka K, et al (2016). Negative influence of programmed death-1-ligands on the survival of esophageal cancer patients treated with chemotherapy. *Cancer Sci* **107**(6), 726–733.

[6] Omloo JM, et al (2007). Extended transthoracic resection compared with limited transhiatal resection for adenocarcinoma of the mid/distal esophagus: five-year survival of a randomized clinical trial. *Ann Surg* **246**(6), 992–1001.

[7] Lerut TE, et al (1994). Advanced esophageal carcinoma. *World J Surg* **18**(3), 379–387.

[8] Waterman TA, et al (2004). The prognostic importance of immunohistochemically detected node metastases in resected esophageal adenocarcinoma. *Ann Thorac Surg* **78**(4), 1161–1169.

[9] Li B, et al (2017). Extended right thoracic approach compared with limited left thoracic approach for patients with middle and lower esophageal squamous cell carcinoma: three-year survival of a prospective, randomized, *Open-label Trial*. *Ann Surg*.

[10] Kayani B, et al (2011). Lymph node metastases and prognosis in oesophageal carcinoma – a systematic review. *Eur J Surg Oncol* **37**(9), 747–753.

[11] van Rossum PS, et al (2013). Imaging strategies in the management of oesophageal cancer: what's the role of MRI? *Eur Radiol* **23**(7), 1753–1765.

[12] Gillies RJ, Kinahan PE, and Hricak H (2015). Radiomics: images are more than pictures, they are data. *Radiology* **278**(2), 563–577.

[13] Yip SS and Aerts HJ (2016). Applications and limitations of radiomics. *Phys Med Biol* **61**(13), R150.

[14] Zhou M, et al (2014). Radiologically defined ecological dynamics and clinical outcomes in glioblastoma multiforme: preliminary results. *Transl Oncol* **7**(1), 5–13.

[15] Aerts HJ, et al (2014). Decoding tumour phenotype by noninvasive imaging using a quantitative radiomics approach. *Nat Commun* **5**.

[16] Coroller TP, et al (2017). Radiomic-based pathological response prediction from primary tumors and lymph nodes in NSCLC. *J Thorac Oncol* **12**(3), 467–476.

[17] Huang Y-q, et al (2016). Development and validation of a radiomics nomogram for preoperative prediction of lymph node metastasis in colorectal cancer. *J Clin Oncol* **34**(18), 2157–2164.

[18] Yip C, et al (2015). Assessment of changes in tumor heterogeneity following neoadjuvant chemotherapy in primary esophageal cancer. *Dis Esophagus* **28**(2), 172–179.

[19] Yushkevich PA, et al (2006). User-guided 3D active contour segmentation of anatomical structures: significantly improved efficiency and reliability. *Neuro-Image* **31**(3), 1116–1128.

[20] Haralick RM and Shanmugam K (1973). Textural features for image classification. *IEEE Trans Syst Man Cybern* **3**(6), 610–621.

[21] Galloway MM (1975). Texture analysis using gray level run lengths. *Comput Graph Image Process* **4**(2), 172–179.

[22] Ganeshan B, et al (2012). Tumour heterogeneity in oesophageal cancer assessed by CT texture analysis: preliminary evidence of an association with tumour metabolism, stage, and survival. *Clin Radiol* **67**(2), 157–164.

[23] Tibshirani R (1996). Regression shrinkage and selection via the lasso. *J R Stat Soc Ser B Methodol* , 267–288.

[24] Friedman J, Hastie T, and Tibshirani R (2010). Regularization paths for generalized linear models via coordinate descent. *J Stat Softw* **33**(1), 1.

[25] Harrell Jr FE (2008). Hmisc: harrell miscellaneous. R package version; 2008. 1(2).

[26] Canty A and Ripley B (2012). boot: Bootstrap R (S-Plus) functions. R package version; 2012. 1(7).

[27] Pencina MJ, D'Agostino RB, and Steyerberg EW (2011). Extensions of net reclassification improvement calculations to measure usefulness of new biomarkers. *Stat Med* **30**(1), 11–21.

[28] Vickers AJ, et al (2008). Extensions to decision curve analysis, a novel method for evaluating diagnostic tests, prediction models and molecular markers. *BMC Med Inform Decis Mak* **8**(1), 53.

[29] Harrell F (2015). Regression modeling strategies: with applications to linear models, logistic and ordinal regression, and survival analysis. Springer; 2015.

[30] Ng F, et al (2013). Assessment of primary colorectal cancer heterogeneity by using whole-tumor texture analysis: contrast-enhanced CT texture as a biomarker of 5-year survival. *Radiology* **266**(1), 177–184.

[31] Okabayashi K, et al (2012). Cancer-testis antigen BORIS is a novel prognostic marker for patients with esophageal cancer. *Cancer Sci* **103**(9), 1617–1624.

[32] Van Vliet E, et al (2008). Staging investigations for oesophageal cancer: a meta-analysis. *Br J Cancer* **98**(3), 547–557.

[33] Khullar OV, et al (2015). Transthoracic versus transhiatal resection for esophageal adenocarcinoma of the lower esophagus: A value-based comparison. *J Surg Oncol* **112**(5), 517–523.

[34] Hulscher JB, et al (2002). Extended transthoracic resection compared with limited transhiatal resection for adenocarcinoma of the esophagus. *N Engl J Med* **347**(21), 1662–1669.

[35] Mao Y, et al (2013). Nationwide speaking tour of standardized diagnosis and treatment for esophageal cancer. *Zhonghua Wei Chang Wai Ke Za Zhi* **16**(9), 801–804.

[36] Tachimori Y (2017). Pattern of lymph node metastases of squamous cell esophageal cancer based on the anatomical lymphatic drainage system: efficacy of lymph node dissection according to tumor location. *J Thorac Dis* **9**(Suppl. 8), S724–S730.

[37] Salminen JT, et al (1999). Endoscopic ultrasonography in the preoperative staging of adenocarcinoma of the distal oesophagus and oesophagogastric junction. *Scand J Gastroenterol* **34**(12), 1178–1182.

[38] Räsänen JV, et al (2003). Prospective analysis of accuracy of positron emission tomography, computed tomography, and endoscopic ultrasonography in staging of adenocarcinoma of the esophagus and the esophagogastric junction. *Ann Surg Oncol* **10**(8), 954–960.

[39] Luketich JD, et al (1997). Minimally invasive surgical staging is superior to endoscopic ultrasound in detecting lymph node metastases in esophageal cancer. *J Thorac Cardiovasc Surg* **114**(5), 817–823.

[40] Van Westreenen H, et al (2004). Systematic review of the staging performance of 18F-fluorodeoxyglucose positron emission tomography in esophageal cancer. *J Clin Oncol* **22**(18), 3805–3812.